MATERIALS CHEMISTRY FRONTIERS

FeP Nanoparticles: A New Material for Microwave Absorption

Journal:	*Materials Chemistry Frontiers*
Manuscript ID	QM-RES-01-2018-000003.R1
Article Type:	Research Article
Date Submitted by the Author:	23-Mar-2018
Complete List of Authors:	Green, Michael; University of Missouri - Kansas City, Chemistry Tian, Lihong; University of Missouri - Kansas City, Xiang, Peng; China Three Gorges University, Murowchick, James; Uniersity of Missouri-Kansas City, Geosciences Tan, Xinyu; China Three Gorges University Chen, Xiaobo; University of Missouri - Kansas City, Chemistry

Journal Name

ARTICLE

FeP Nanoparticles: A New Material for Microwave Absorption

Michael Green,[a] Lihong Tian,[a,b] Peng Xiang,[c] James Murowchick,[d] Xinyu Tan,[c,*] and Xiaobo Chen[a,*]

Received 00th January 20xx,
Accepted 00th January 20xx

DOI: 10.1039/x0xx00000x

www.rsc.org/

Microwave absorbing materials play a critical role within the realms of information and homeland security in times of both peace and international conflicts; as such, discovering new materials for microwave absorption is of critical importance due to their applications in civil and military technologies. In this study, we report for the first time FeP nanoparticles as a promising material for microwave absorption. The FeP nanoparticles, fabricated through a facile thermal phosphorization process, display impressive microwave absorbing performance with a reflection loss of -37.68 dB at 13.6 GHz, indicating a large absorption efficiency over 99.9%. As the thickness of the microwave absorber increases from 1.0 to 6.0 mm, the microwave absorbing peak frequency (f_{max}) shifts to the lower frequency monotonically, and the critical absorbing peak width (Δf_{10}: peak width at RL = -10 dB) increases monotonically, while the reflection loss stays below -33.0 dB. This indicates a robust performance across a tunable frequency range from 8.86 to 15.1 GHz for microwave absorption. These characteristics demonstrate that FeP nanoparticles may act as a new and promising microwave absorbing material.

Introduction

As conflicts between intellectual powers continue to place the global community in a continuous state of peril, the protection of homelands and citizens has become a much more challenging task for those countries involved in the struggle to assert their national sovereignty and international dominance. As a consequence, global players continue to rely on cyber security and advanced technologies for defensive protection. Meanwhile, the recent reporting of information leaking has exposed the current state of security as lacking, and now exclaims a sort of necessity for the continued innovation within the realm of information protection. Thus, the development of more sophisticated and higher quality microwave absorbing or radar shielding materials provides one potential solution to several of the nuanced sub-problems at hand. These materials have been utilized to effectively protect information in transport across a physical domain as well as safeguard warships and aircrafts through stealth. For example, the outside of the devices or equipment can be coated with microwave absorbing materials to reduce the electromagnetic interference between electrical components and circuits in many electronics, and to reduce the radar reflecting signature of aircraft, warships and tanks. [1-3] Therefore, discovering materials with good microwave absorbing properties is a top priority in our quest to effectively protect our welfare and national security.

So far, various materials and composites have been explored for microwave absorption, including single-walled and multi-walled carbon nanotubes (CNTs),[3-9] graphite,[10] carbon fiber,[11] carbon black,[9] graphene,[12-13] conducting polymers,[14,15] C-Sn,[16] Fe_3O_4,[17,18] MnO_2,[19] $BaTiO_3$/polyaniline,[20] Ag-$Ni_{0.5}Zn_{0.5}Fe_2O_4$,[21] $BaCe_{0.05}Fe_{11.95}O_{19}$,[22] $(Li_{0.5}Fe_{0.5})_{0.7}Zn_{0.3}Fe_2O_4$,[23] $MnFe_2O_4$,[14] $MnFe_2O_4$–TiO_2,[24] et al. Microwave absorbing materials are normally categorized into carboneous materials and ferrite materials, and the main mechanisms are dipole rotations and magnetic domain resonance. The phenomena is overall due to the dielectric and magnetic losses upon the interaction with the incident microwave electromagnetic fields within those given materials. For example, Zhao et al. studied the microwave absorption, and complex permittivity and permeability of epoxy composites containing Ni-coated and Ag nanowires filled carbon nanotubes, and found that the microwave absorption enhancement of Ni-coated CNTs/epoxy composites is attributed to the dielectric and magnetic losses within the composite, and the microwave absorption of Ag nanowire-filled CNTs/epoxy composites is mainly attributed to the dielectric loss rather than the magnetic loss.[3] Yusoff et al. found that the microwave absorbing properties of $(Li_{0.5}Fe_{0.5})_{0.7}Zn_{0.3}Fe_2O_4$ is improved with the addition of CuO and MgO.[23] Chen et al. reported that a broadband and tunable high-performance microwave absorption can be achieved with ultralight and highly compressible graphene foams. These examples are just some of the reports that represent the exciting progress in this field of microwave absorbing materials.[12] Fe-encapsulated CNTs and CNTs of different helicities have been reported with excellent microwave absorption performance of with.[25-27]

[a] Department of Chemistry, University of Missouri – Kansas City, MO 64110, USA.
[b] Hubei Collaborative Innovation Center for Advanced Organochemical Materials, Ministry of Education Key Laboratory for the Synthesis and Applications of Organic Functional Molecules, Hubei University, Wuhan 430062, China.
[c] College of Materials and Chemical Engineering, Hubei Provincial Collaborative Innovation Center for New Energy Microgrid, China Three Gorges University, Yichang, 443002, China.
[d] Department of Geosciences, University of Missouri – Kansas City, MO 64110, USA.
* Email: tanxin@ctgu.edu.cn, chenxiaobo@umkc.edu.

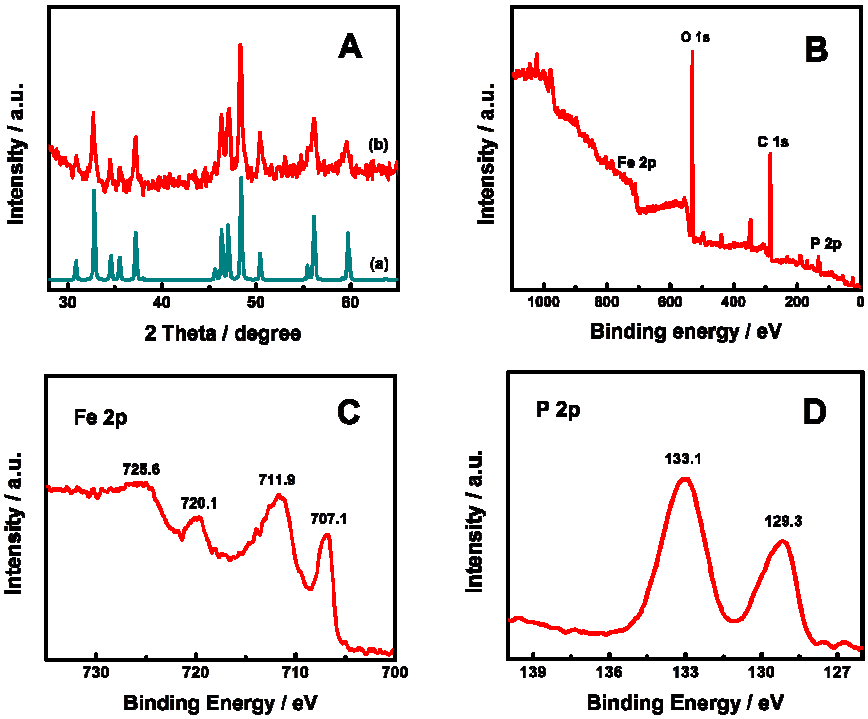

Figure 1. (A) XRD patterns of (a) the FeP nanoparticles and (b) the FeP standard (JCPDF no 65-2595), (B) XPS survey, (C) Fe 2p core-level, and (D) P 2p core-level XPS spectra of the FeP nanoparticles.

Different from those carboneous or ferrite materials, we have recently found that simple oxide materials, such as TiO_2[28-31] and ZnO,[31] as well as complex dielectric oxides such as $BaTiO_3$[32] nanoparticles, can possess impressive microwave absorption performances after their dielectric properties are largely modified by hydrogenation (heating under a hydrogen-containing environment) at elevated temperatures, via the perturbation of their lattice structures and defect formation, which induces apparent charge accumulation in the crystalline/disordered interfaces and the materials internal electric field.[33] To explain the improvement in overall microwave absorption performance of those hydrogenated nanoparticles, we proposed the so-called collective-movement-of-interfacial-dipole mechanism (CMID), where the dipoles across the crystalline/disordered interfaces can "echo" with the incident electromagnetic field, so to amplify the microwave absorption, in an analogy to the plasmonic resonance on the surface of metallic nanoparticles. Despite of those exciting discoveries, new microwave absorption materials are highly needed, as every material seems to offer some unique advantages and disadvantages intrinsic to the material, and thus may be suitable only for microwave absorption applications within certain frequency ranges. Recently, many excellent strategies have been developed in making monodispersed nanoparticles.[34-38]

This study reports for the first time that FeP nanoparticles are a promising material for microwave absorption application. FeP has recently been reported as a promising electrocatalyst for hydrogen production from electrochemical water splitting and as such has attracted much attention.[39-41] For example, Callejas et al. found that the FeP/Ti had a small overpotential of 50 mV to reach a benchmark current density of 10 mA cm^{-2} in 0.5 M H_2SO_4 of electrochemical hydrogen evolution reaction,[41] where the FeP was obtained by reacting $Fe(CO)_5$ with trioctylphosphine in mixed oleylamine and 1-octadecene.[41] We recently reported that uncapped FeP nanoparticles can be synthesized by reacting Fe_2O_3 with NaH_2PO_2,[39] with satisfied activity for hydrogen evolution reaction.[39] Here, we report that FeP nanoparticles also have an impressive capacity for microwave absorption. A large reflection loss of -37.68 dB can be observed at 13.6 GHz, which correlates to an absorption efficiency of over 99.9%. Meanwhile, the microwave absorbing peak frequency (f_{max}) can be adjusted as a function of the thickness of the FeP absorber. For example, f_{max} can be tuned from 15.1 to 8.86 GHz as the thickness increases from 1.0 to 6.0 mm, while maintaining a high reflection loss below -33.0 dB (absorption efficiency over 99.9%). As such, FeP nanoparticles demonstrate as a new material for microwave absorption, but also show a great promise as a high-performance material for microwave absorption due to its potential to be fine-tuned.

Results and discussion

Figure 1 showed the X-ray diffraction (XRD) patterns of the FeP nanoparticles with the FeP standard (JCPDF no 65-2595). The

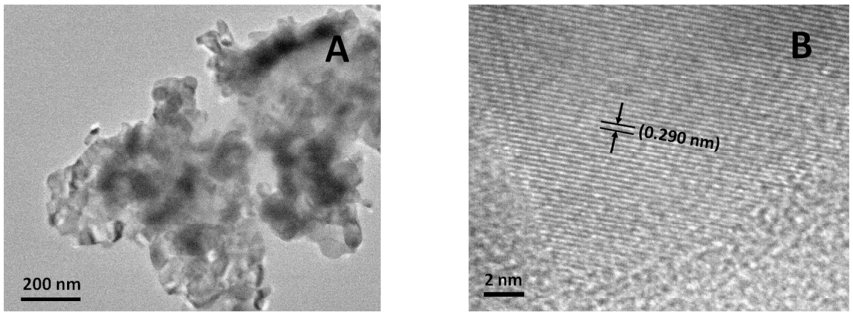

Figure 2. (a) TEM and (b) HRTEM images of FeP nanoparticles.

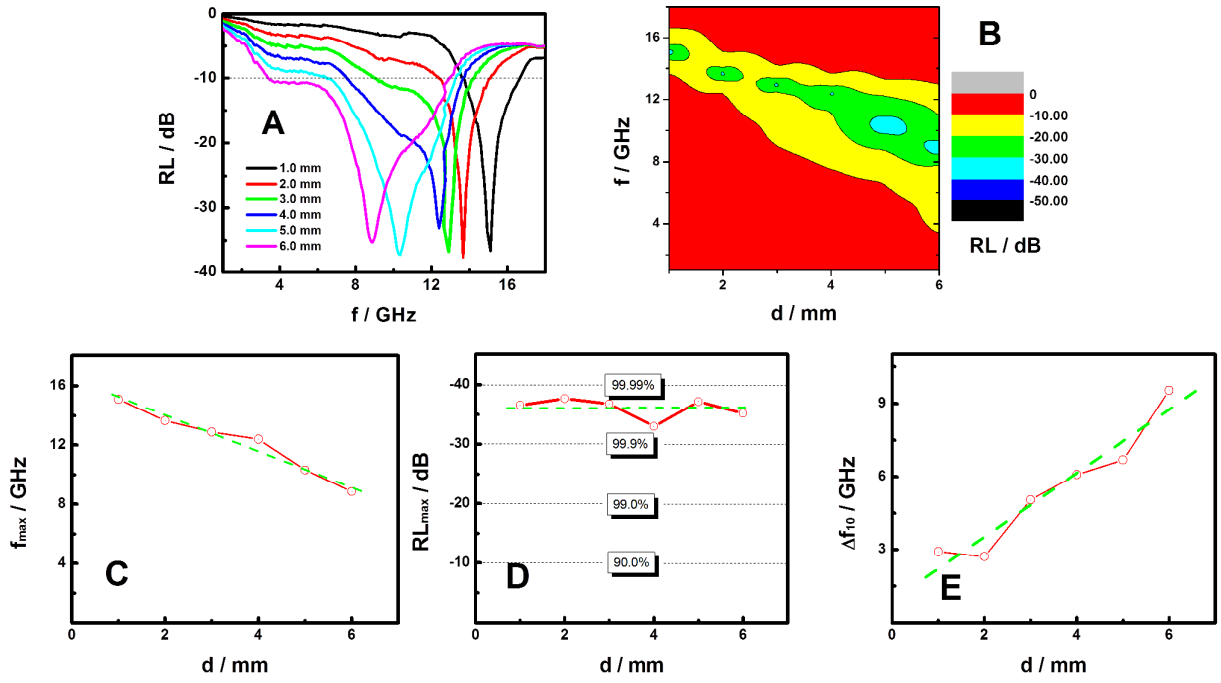

Figure 3. (A) The RL curves of the FeP nanoparticle absorbers in the frequency range of 1.0-18.0 GHz, (B) The relationships of the microwave absorbing peak frequency (f_{max}/ GHz), (C) the maximum absorbing peak value (RL_{max} / dB) and (D) the critical absorbing peak width (Δf_{10}/GHz) with the thickness (d/mm) of the FeP nanoparticle absorbers. The dashed green lines in (B)-(D) are the visual guidelines.

well-matched diffraction patterns indicated the successful formation of FeP nanoparticles. The sharp diffraction peaks suggest that the FeP nanoparticles were highly crystallized. The average crystalline size was about 26.1 nm, estimated with the Scherrer equation, using the diffraction (011) and (211) peaks at 32.78 and 48.37°, respectively. These FeP nanoparticles were obtained through a thermal phosphorization process based upon our previous work.[39] Briefly, α-Fe_2O_3 and $NaH_2PO_2{\cdot}H_2O$ were heated in argon at 350 °C for 3h, then washed in HCl and dried at 100 °C. The high-temperature phosphorization reaction of α-Fe_2O_3 with the PH_3 gas produced from NaH_2PO_2 allowed the formation of highly crystalline FeP nanoparticles.[39]

The X-ray photoelectron spectroscopy (XPS) survey spectrum in Figure 1B revealed that Fe, P, O and C elements were present in the FeP nanoparticles. The oxygen is potentially related to ferric hydroxides/oxides, or absorbed water on the surface. The two peaks at 707.1 and 720.1 eV in the Fe 2p spectrum in Figure 1C correlate to the $2p_{3/2}$ and $2p_{1/2}$ of Fe^{3+} ions in the FeP;[39] the other two peaks at 711.9 and 725.6 eV were likely from the $2p_{3/2}$ and $2p_{1/2}$ of Fe^{3+} ions likely in the form of FeO(OH) on the surface of the FeP nanoparticles.[39] The peaks at 129.3 and 133.1 eV in the P 2p spectrum in Figure 1D were from the $2p_{3/2}$ and $2p_{1/2}$ of P^{3-} ions in the FeP nanoparticles.[39]

The transmission electron microscopy (TEM) image (Figure 2A) shows that the FeP nanoparticles were aggregated with a

primary particle size of about 50 to 60 nm. As the average crystalline size was about 26.1 nm based on the XRD analysis, each particle had 2-3 crystalline domains. The high-resolution transmission electron microscopy (HRTEM) image (Figure 2B) displayed clear lattice fringes with spacing value of 0.290 nm from the (002) crystal plane of the FeP nanoparticles, indicating the high crystallinity of the FeP nanoparticles.

Figure 3A shows the reflection loss (RL) curves of the FeP nanoparticles in the frequency range of 1.0-18.0 GHz. The FeP nanoparticles were embedded in paraffin wax for the measurements. Paraffin wax is transparent in the testing frequency range and does not have much absorption.[3] As demonstrated for all samples tested with thickness between 1.0 to 6.0 mm, a large reflection loss peak is observed with minimal values between -30 and -40 dB, and sizable sections of the tested frequency range are below -10 dB. RL of -10 dB means that reflection loss is 90% is observed, and RL of -30 and -40 dB means reflection loss is 99.9 and 99.99 percent, respectively. In other words, RL of -10 dB indicates that absorption is 90%, and RL of -30 and -40 dB means absorption is 99.9 and 99.99%. As such Figure 3A indicates that the FeP nanoparticles demonstrate a very impressive overall microwave absorbing performance. The 2D contour plot of the RL vs. f & d in Figure 3B clearly demonstrates the evolution of the microwave absorption as the frequency and thickness vary.

To better understand the microwave absorption performance of FeP nanoparticles, Figure 3C displays the relationship between the microwave absorbing peak frequency (f_{max} / GHz) and the thickness (d/ mm) of the FeP nanoparticle absorbers. Clearly, as the thickness increases, the peak frequency shifts to lower values. Specifically, as the thickness of the absorber increased from 1.0 to 6.0 mm, the peak frequency decreased almost linearly from 15.1 to 8.86 GHz, as can be seen from the straight dashed green line shown in the graph.

The relationships between the maximum absorbing peak value (RL_{max} / dB) and the thickness (d/ mm) is shown in Figure 3D. Apparently, all the FeP absorbers under test with the thickness between 1.0 and 6.0 mm have a RL_{max} value between -30 and -40 dB, or an maximal absorption efficiency between 99.9 and 99.99 percent. This indicates that as long as those FeP nanoparticles are prepared with a thickness within such a range, good microwave absorption efficiency would be readily achieved. This characteristic gives us a large flexibility and feasibility in coating a target surface without worrying so much on the fine controls of the thickness to meet an absorbing capability requirement, because more commonly, a small change of the thickness of the absorbing material will largely affect the efficiency of the absorption.[3-24]

Figure 3E displays the relationship between the critical absorbing peak width (Δf_{10} / GHz) and the thickness (d/ mm) of the FeP nanoparticle absorbers. Here, the RL of -10 dB is used as a critical value, as it indicates that 90% of the incident microwave electromagnetic field is effectively neutralized with respect to detection. Therefore, the frequency range with RL value of -10 dB or more is expressed as the critical absorbing peak width (Δf_{10} / GHz). The larger the Δf_{10} width, the more useful the coating is, as it can shield microwave irradiation in a broader frequency range.

As shown in Figure 3E, when the thickness of the absorber becomes bigger, the critical absorbing peak width (Δf_{10} / GHz) increases in pseudo-linear fashion. Specifically, Δf_{10} was enhanced from about 2.90 to 9.60 GHz as the thickness rose

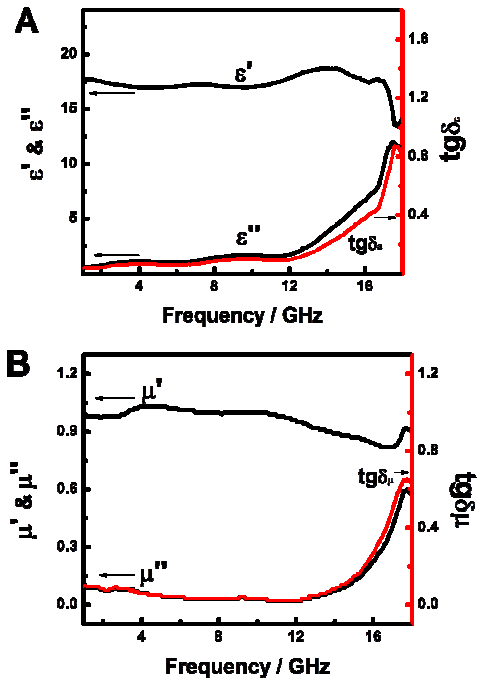

Figure 4. (A) The complex permittivity (ε', ε", $tg\delta_\varepsilon$) and (B) complex permeability (μ', μ", $tg\delta_\mu$) of FeP nanoparticles in the frequency range of 1.0-18.0 GHz.

from 1.0 to 6.0 mm. This indicates that the thickness of the FeP microwave absorber could be used to effectively expand the effective shielding frequency range.

To further understand the microwave absorption performance of the FeP nanoparticles, their dielectric and magnetic properties are analyzed, as they are related to the reflection loss (RL) value through the following equations:

$$RL(dB) = 20 \log |(Z_{in} - Z_0)/(Z_{in} + Z_0)| \quad (1)$$

$$Z_{in} = Z_0(\mu_r/\varepsilon_r)^{1/2}\tanh[j(2\pi fd/c)(\mu_r\varepsilon_r)^{1/2}] \quad (2)$$

where RL(dB) is the reflection loss in dB, Z_{in} the input impedance of the absorber, Z_0 the impedance of free space, μ_r the relative complex permeability, ε_r relative complex permittivity, f is the frequency of the electromagnetic wave, d the thickness of the absorber and c the velocity of light.[30-32]

Figure 4A shows the complex permittivity (ε', ε", $tg\delta_\varepsilon$) of the FeP nanoparticles in the frequency range of 1.0-18.0 GHz. The ε' value starts with 17.7 at 1.0 GHz, gradually increases to 18.7 at 14.1 GHz and then decreases to 14.0 at 18.0 GHz; the ε" climbs slowly from 0.62 at 1.0 GHz to 1.76 at 12.0 GHz and then quickly shoots up to 11.5 at 18.0 GHz; $tg\delta_\varepsilon$ gradually changes from 0.03 at 1.0 GHz to 0.10 at 12.0 GHz and then

quickly soars to 0.81 at 18.0 GHz, with a similar trend as the ε". ε', ε" and $tg\delta_\varepsilon$ =ε"/ε' reflect the stored, lost electrical energy and the power lost ratio within the medium. The above results suggest that the FeP nanoparticles have an increasing stored electrical energy as the frequency of the incident electromagnetic field increased. This seems to indicate that, as the frequency of the incident field is increased, the echoes of the electric field, or dipoles in the FeP nanoparticles to the oscillating field, were catching up quicker. The intensification of ε" and $tg\delta_\varepsilon$ as a function of frequency suggests that the consumed electrical energy also increased with respect to said frequency.

The permeability parameters (μ', μ", and $tg\delta_\mu$) of the FeP nanoparticles are shown in Figure 4B. The μ' increases from 0.99 at 1.0 GHz to 1.03 at 4.5 GHz, then decreases to 0.82 at 16.8 GHz and finally climbs to 0.91 at 18.0 GHz; the μ" decreases from 0.09 at 1.0 GHz to 0.02 at 12.0 GHz and then rises to 0.57 at 18.0 GHz; $tg\delta_\mu$ starts with 0.09 at 1.0 GHz and gradually declines to 0.02 at 12.0 GHz, only to then surge to 0.63 at 18.0 GHz. The change of $tg\delta_\mu$ with respect to the frequency matches well with that of μ" with the frequency. Since μ', μ"and $tg\delta_\mu$ (which is μ"/μ') reflect the stored magnetic energy, lost magnetic energy, and the power lost ratio within the medium, these results suggest that the stored magnetic energy slightly spirals up with the frequency from 1.0 to 12.0 GHz, but then falls off from 12.0 to 16.8 GHz, only to subsequently reclimb from 16.8 to 18.0 GHz, while the lost magnetic energy and the magnetic power lost ratio drop slightly from 1.0 to 12.0 GHz, but then rises from 12.0 to 18.0 GHz. From Figures 4A and 4B, we can see that both ε" (and $tg\delta_\varepsilon$) and μ" (and $tg\delta_\mu$) grew slowly from 1.0 to 12.0 GHz, but rocketed rapidly from 12.0 to 18.0 GHz.

In order to understand the microwave absorption performance of the FeP nanoparticles, we have further examined their electrical conductivity (σ) and the skin-depth (δ) of the microwave irradiation in the FeP nanoparticles. The σ curve in the frequency range of 1-18 GHz is shown in Figure 5A. The σ is calculated with $\sigma\,(S/m) = 2\pi f\varepsilon_0\varepsilon''$, where ε_0 is the free space permittivity (8.854×10^{-12} F/m), f is the frequency (Hz), and ε" is the imaginary component of permittivity.[1,42] σ increases gradually from 0.03 to 1.08 S/m as the frequency changes from 1.0 to 12.0 GHz and then to 11.56 S/m at 18.0 GHz. The σ values indicate that the FeP nanoparticles have a good electrical conductivity in the microwave frequency, or in another word, there is an efficient electrical relaxation channel for the incoming microwave irradiation in the FeP nanoparticles, which allows the decay of the microwave irradiation as it enters the FeP nanoparticles. This is verified with the δ curve of the microwave irradiation as shown in Figure 5B. The δ value is calculated with $(\delta\ /\ m) = (\pi f\mu_0\mu_r\sigma)^{-1/2}$, where μ_0 is the permeability of free space ($4\pi \times 10^{-7}$ H/m), μ_r is the relative permeability, and σ is the electrical conductivity (S/m).[1,42] δ decreases monotonically from 78.18 to 4.56 mm as the frequency increases from 1.0 to 18.0 GHz. The δ value indicates how deep the microwave irradiation needs to go inside the materials to get its intensity decayed to 1/e times. The small δ values at larger frequency ranges indicates that the microwave irradiation with higher frequency decays faster inside the FeP nanoparticles, consistent with the large RL values in the higher frequency range.

On the other hand, as shown in eqn. 1, the RL is largely controlled by Z_{in} - the input impedance of the absorber which itself depends on $(\mu_r/\varepsilon_r)^{1/2}$, $(\mu_r\varepsilon_r)^{1/2}$ and d – the thickness of the absorber (eqn. 2). Our studies show that RL is determined by the coplay of those three major variables. A good match of μ_r, ε_r and d is commonly believed to ultimately determine the efficiency of a given microwave absorber.[3-24] As seen from Figures 4A and 4B, μ_r and ε_r in the frequency range change in the opposite directions as the frequency changed, but in the high frequency range, they change in the same direction. Such suggests that $(\mu_r\varepsilon_r)^{1/2}$ has a small variation in the lower

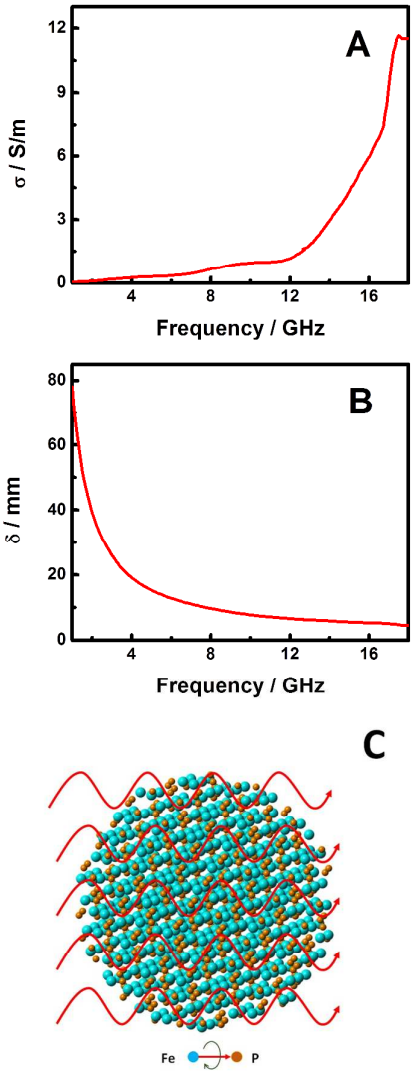

Figure 5. (A) σ and (B) δ curve of the FeP nanoparticles in the frequency range of 1.0-18.0 GHz. (C) A schematic illustration of the microwave absorption of FeP nanoparticles.

frequency range but a large value in the higher frequency range, while $(\mu_r/\varepsilon_r)^{1/2}$ has an opposite trend. Since the effective microwave absorption mainly occurs in the high frequency range, this observation indicates that the product of μ_r and ε_r ($\mu_r\varepsilon_r$) might play a big role in the microwave absorption of FeP nanoparticles. Meanwhile, as the thickness of the FeP absorber is increased from 1.0 to 6.0 mm, the overall RL is maintained as constant. This indicates that the thickness may not play a big role in the efficiency of the absorption, so long as the thickness is larger than some critical value. Figure 5C displays the schematic illustration of the microwave absorption mechanism of the FeP nanoparticles. As the microwave irradiation encounters the FeP nanoparticles, it echoes with polar rotations and likely with some magnetic domain resonance. The existence of the polar rotations can be seen from the large $tg\delta_\varepsilon$ and σ values which indicate the efficient electrical relaxation of the microwave irradiation inside the FeP nanoparticles. Similarly, the existence of the magnetic domain resonance can be foreseeable based on the large $tg\delta_\mu$ values, especially at higher frequencies. The sources of the polar rotations can be traced backed to the apparently polar Fe-P bonds, the asymmetrical lattice structure of the FeP nanoparticles, and apparent asymmetrical structure on the surface and in the interfaces between adjacent nanoparticles, causing internal and interfacial polarization. The sources of the magnetic resonance can be understood in that there are unpaired electrons in the Fe^{3+} 3d orbitals which can apparently induce spin states to echo with the incoming electromagnetic field of the microwave irradiation. The efficient decay of the microwave irradiation can be seen from small δ value and the large RL curves. As shown in Figure 3B and 3D, a thicker absorber can shift the absorbing frequency to a lower frequency, as well as widen the absorbing ranges, therefore making the FeP nanoparticles both a promising and tunable microwave absorbing material.

Conclusions

In summary, we have shown for the first time that FeP nanoparticles prepared through a thermal phosphorization process display large microwave reflection losses and high absorption performance. A large reflection loss of -37.68 dB at 13.6 GHz has been obtained with a large absorption efficiency of over 99.9%. Furthermore, the thickness of the FeP nanoparticle microwave absorber can be used to tune both the microwave absorbing peak frequency (f_{max}) between 15.1 and 8.86 GHz and the critical absorbing peak width (Δf_{10}: peak width at RL = -10 dB), while keeping a large reflection loss below -30.0 dB to maintain a high absorbing performance. These characteristics thus show FeP nanoparticles as a new and promising microwave absorbing material.

Experimental

The FeP nanoparticles were obtained through a thermal phosphorization process following our previous work.[31] Briefly, suitable amounts of α-Fe_2O_3 and $NaH_2PO_2{\cdot}H_2O$ were grinded and heated in argon at 350 ^oC for 3h, followed by a thorough wash in HCl and a drying process at 100 ^oC. The crystal structure of the formed FeP nanoparticles was examined on a Rigaku Miniflex X-ray Diffractometer (XRD) with a Cu Kα (λ= 0.15418 nm) radiation source. The morphologies and crystallinity of the FeP nanoparticles were studied with transmission electron microscopy (TEM) and high resolution transmission electron microscopy (HRTEM). XPS data were collected using a Kratos Axis 165 X-ray photoelectron spectrometer with an Al/Mg dual-anode X-ray source, using a photon beam of 1486.6 eV. All the spectra were calibrated to the carbon peak at 284.6 eV from the carbon tape used to fix the sample. The complex permittivity and permeability of the FeP nanoparticles were measured at the frequency range of 1.0–18.0 GHz using HP8722ES network analyzer at room temperature with ring-shape samples containing 60 wt%. nanoparticles dispersed in paraffin wax, which was cast into a ring mold with a thickness of 1.0-6.0 mm, an inner diameter of 3 mm, and an outer diameter of 7 mm. 60wt% was chosen as the concentration in order to keep consistent with other samples in our previous studies.[28-32] The size of the ring was carefully controlled by polishing after the ring was pressed. Parrafin wax was transparent to the microwave irradiation and was commonly used as the dispersing matrix for microwave absorption measurements.

Conflicts of interest

The authors herein declare no such conflicts of interest.

Acknowledgements

X. C. appreciates the support from the U.S. National Science Foundation (DMR-1609061), and the College of Arts and Sciences, University of Missouri-Kansas City. L. T. thanks the National Natural Science Foundation of China (No. 51302072) and China Scholarship Council for their financial supports. X. Tan thanks the support from the National Natural Science Foundation of China (11374181).

Notes and references

1 D. Micheli, *Radar absorbing materials and microwave shielding structures design: By using multilayer composite materials, nanomaterials and evolutionary computation*, LAP LAMBERT Academic Publishing, 2011.
2 Y. Duan and H. Guan, *Microwave absorbing materials*, Pan Stanford, Singapore, 2016.
3 D.-L. Zhao, X. Li and Z.-M. Shen, *Compos. Sci. Technol.*, 2008, **68**, 2902.
4 L. Deng and M. Han, *Appl. Phys. Lett.*, 2007, **91**, 023119.
5 Z. Fan, G. Luo, Z. Zhang, L. Zhou and F. Wei, *Mater. Sci. Eng. B*, 2006, **132**, 85.
6 T. H. Ting, Y. N. Jau and R. P. Yu, *Appl. Surface Sci.*, 2012, **258**, 3184.
7 Z. Liu, G. Bai, Y. Huang, F. Li, Y. Ma, T. Guo, X. He, X Lin, H. Gao and Y. Chen *J. Phys. Chem. C*, 2007**, 111**, 13696.
8 M. H. Al-Saleh and U. Sundararaj *Carbon*, 2009, **47**, 1738.

9 M. H. Al-Saleh, W. H. Saadeh and U. Sundararaj *Carbon*, 2013, **60**, 146 –156.
10 X. Ji, M. Lu, F. Ye and Q. Zhou, *Adv. Mech. Eng. Appl.*, 2012, **3**, 294.
11 T. Zou, N. Zhao, C. Shi and J. Li, *Bull. Mater. Sci.*, 2011, **34**, 75.
12 Y. Zhang, Y. Huang, T. Zhang, H. Chang, P. Xiao, H. Chen, Z. Huang and Y. Chen, *Adv. Mater.*, 2015, **27**, 2049.
13 X. Bai, Y. Zhai and Y. Zhang, *J. Phys. Chem. C,* 2011, **115**, 11673.
14 L. Olmedo, P. Hourquehie and F. Jousse, *Adv. Mater.*, 1993, **5**, 373.
15 P. Chandrasekhar and K. Naishadham, *Synth. Metals*, 1999, **105,** 115.
16 Z. H. Wang, Z. Han, D. Y. Geng and Z. D. Zhang, *Chem. Phys. Lett.*, 2010, **489**, 187.
17 O. Chiscan, I. Dumitru, P. Postolache, V. Tura and A. Stancu, *Mater. Lett.*, 2012, **68**, 251.
18 A. Yan, Y. Liu, Y. Liu, X. Li, Z. Lei and P. Liu, *Mater. Lett.*, 2012, **68**, 402.
19 B. Lan, M. Sun, T. Lin, G. Cheng, L. Yu, S. Peng and J. Xu, *Mater. Lett.*, 2014, **121**, 234.
20 C. C. Yang, Y. J. Gung, W. C. Hung, T. H. Ting and K. H. Wu, *Compos. Sci. Technol.*, 2010, **70**, 466.
21 C.-H. Peng, H.-W. Wang, S.-W. Kan, M.-Z. Shen, Y.-M. Wei and S.-Y. Chen, *J. Magn. Magn. Mater.*, 2004, **284**, 113.
22 C. Sun, K. Sun and P. Chui, *J. Magn. Magn. Mater.*, 2012, **324**, 802.
23 A. N. Yusoffa and M. H. Abdullah, *J. Magn. Magn. Mater.*, 2004, **269**, 271.
24 H.-M. Xiao, X.-M. Liu and S.-Y. Fu, *Comp. Sci. Technol.*, 2006, **66**, 2003.
25 R. C. Che, L.-M. Peng, X. F. Duan, Q. Chen and X. L. Liang, *Adv. Mater.* 2004, **16**, 401.
26 X. Qi, J. Xu, Q. Hu, W. Zhong and Y. Du, *Mater. Sci. Eng. B*, 2015, **198**, 108.
27 X. Qi, Y. Yang, W. Zhong, Y. Deng, C. Au and Y. Du, *J. Solid State Chem.* 2009, **182**, 2691.
28 T. Xia, C. Zhang, N. A. Oyler and X. Chen, *Adv. Mater.*, 2013, **25**, 6905.
29 T. Xia, C. Zhang, N. A. Oyler and X. Chen, *J. Mater. Res.*, 2014, **29**, 2198.
30 L. Tian, J. Xu, M. Just, M. Green, L. Liu and X. Chen, *J. Mater. Chem. C*, 2017, **5**, 4645.
31 T. Xia, Y. Cao, N. A. Oyler, J. Murowchick, L. Liu and X. Chen, *ACS Appl. Mater. Interfaces*, 2015, **7**, 10407.
32 L. Tian, X. Yan, J. Xu, P. Wallenmeyer, J. B. Murowchick, L. Liu and X. Chen, *J. Mater. Chem. A,* 2015, **3**, 12550.
33 J. Dong, R. Ullal, J. Han, S. Wei, X. Ouyang, J. Dong and W. Gao, *J. Mater. Chem. A*, 2015, **3**, 5285.
34 Y. Chen, D. Yang, Y. J. Yoon, X. Pang, Z. Wang, J. Jung, Y. He, Y. W. Harn, M. He, S. Zhang, G. Zhang and Z. Lin, *J. Am. Chem. Soc.* 2017, **139**, 12956.
35 Y. Chen, Y. Yoon, X. Pang, Y. He, J. Jung, C. Feng,, G Zhang and Z. Lin, *Small* 2016, **12**, 6714.
36 C. Feng, X. Pang, Y. He, Y. Chen, G. Zhang and Z. Lin, *Polym. Chem.* 2015, **6**, 5190.
37 X. Liu, J. Ioccozia, Y. Wang, X. Cui, Y. Chen, S. Zhao, Z. Li and Z. Lin, *Energy Environ. Sci.*, 2017, **10**, 402.
38 X. Li, J. Iocozzia, Y. Chen, S. Zhao, X. Cui, W. Wang, H. Yu, S. Lin and Z. Lin, *Angew. Chem.-Int. Ed.* 2018, **57**, 2046.
39 L. Tian, X. Yan and X. Chen, *ACS Catal.*, 2016, **6**, 5441.
40 Y. Xu, R. Wu, J. Zhang, Y. Shi and B. Zhang, *Chem. Commun.*, 2013, **49**, 6656.
41 J. F. Callejas, J. M. McEnaney,; C. G. Read, J. C. Crompton, A. J. Biacchi, E. J. Popczun, T. R. Gordon, N. S. Lewis and R. E. Schaak, *ACS Nano*, 2014, **8**, 11101.
42 M. Green, L. Tian, P. Xiang, J. Murowchick, X. Tan and X. Chen, *Mater. Today Nano*, accepted.